This is the peer reviewed version of the following article: Phys.Chem.Chem.Phys.,2010,12, 4287–4290, which has been published in final form at https://doi.org/10.1039/B924306M . For terms of use of this PostPrint see homepage of the Royal Society of Chemsitry.

Is there a Au-S bond dipole in self-assembled monolayers on gold?

LinJun Wang,[a,c] Gerold M. Rangger,[b] ZhongYun Ma,[c] QiKai Li,[c] Zhigang Shuai,*[a,c] Egbert Zojer,*[b] and Georg Heimel[d]

Received (in XXX, XXX) Xth XXXXXXXXX 200X, Accepted Xth XXXXXXXXX 200X
First published on the web Xth XXXXXXXXX 200X
DOI: 10.1039/b000000x

Self-assembled monolayers (SAMs) of functionalized thiols are widely used in organic (opto)electronic devices to tune the work function, Φ, of noble-metal electrodes and, thereby, to optimize the barriers for charge-carrier injection. The achievable Φ values not only depend on the intrinsic molecular dipole moment of the thiols but, importantly, also on the bond dipole at the Au-S interface. Here, on the basis of extensive density-functional theory calculations, we clarify the ongoing controversy regarding the existence, the magnitude, and the nature of that bond dipole.

The work function, Φ, of a metal is defined as the energy difference between its Fermi level, E_F, and the energy of an electron at rest directly outside the metal surface, E_{vac}. Thus, to modify Φ by an amount $\Delta\Phi$, a SAM must introduce a potential energy step between metal and vacuum. In order to allow for a rational design of molecules that induce a desired $\Delta\Phi$, the latter is commonly split into two additive components: The first, ΔE_{vac}, arises from the molecular ad-layer only and the second, ΔE_{BD}, reflects the interfacial charge rearrangements upon molecule-metal bonding. Disregarding atomic-scale lateral inhomogeneities in the SAM, each potential energy step is linked to a corresponding plane-averaged charge (re)distribution, $\rho(z)$, via the Poisson equation,[1-3]

$$\nabla^2 E(z) = \frac{e}{\varepsilon_0}\rho(z) \qquad (1)$$

where e denotes the (by definition positive) elementary charge and ε_0 the vacuum permittivity. As only a net dipole moment perpendicular to the surface leads to a non-vanishing ΔE, Eq. 1 is commonly replaced by the heuristic Helmholtz equation, where the two contributions to $\Delta\Phi$ are regarded as arising from two laterally homogenous dipole layers.[1-9]

$$\Delta\Phi = \Delta E_{vac} + \Delta E_{BD} = -\frac{en}{\varepsilon_0}\left[\frac{|\mu|\cos(\beta)}{\varepsilon_{eff}(n)} + \mu_{BD}(n)\right] \qquad (2)$$

Here, n denotes the molecular packing density, $|\mu|$ is the dipole moment of the free molecule, and β is the angle between the dipole axes of the molecules in the SAM and the surface normal. Generally, the depolarization factor ε_{eff} and the *bond dipole* at the Au-S interface, μ_{BD}, depend on the coverage in a non-trivial manner,[10] but the same n (full coverage) is assumed for all SAMs considered here.

For many adsorbates, the conceptual partitioning of $\Delta\Phi$ into a purely molecular part (first term in Eq. 2) and a bonding-induced part (second term in Eq. 2) is unambiguously defined.[2] However, for SAMs formed by thiols, two different partitioning schemes appear in literature: For the molecular contribution to $\Delta\Phi$, thiols (*i.e.*, R–SH species) are considered in the first[1-5] and R–S• radical species in the second.[6-9] These correspond to two conceptually different points of view,

$$\text{R–SH} + \text{Au} \rightarrow \text{R–S–Au} + \tfrac{1}{2}\,\text{H}_2 \qquad (3a)$$

$$\text{R–S•} + \text{Au} \rightarrow \text{R–S–Au} \qquad (3b)$$

where the first regards the bonding of the SAM to the metal as *replacing* S–H bonds with S–Au bonds and the second as *forming* new bonds between R–S• radicals and gold. Naturally, appreciably different molecular dipole moments are found for the saturated and the radical species and, consequently, by virtue of Eq. 2, also different ΔE_{vac} values (see ESI†). As, however, the final situation is identical in both approaches, *i.e.*, a thiolate SAM on a gold surface (R–S–Au) with one given $\Delta\Phi$, Eq. 2 implies that then also the bonding-induced contribution to the work-function modification, ΔE_{BD}, must differ between the two approaches. In density-functional theory (DFT) calculations, the latter is obtained by applying Eq. 1 to the plane-averaged charge-density differences, ρ_{diff}, that are associated with the processes indicated in Eqs. 3.[1-3, 9]

$$\rho_{diff}^{sat} = \rho_{sys} - \rho_{Au} - (\rho_{sat} - \rho_{H}) \qquad (4a)$$

$$\rho_{diff}^{rad} = \rho_{sys} - \rho_{Au} - \rho_{rad} \qquad (4b)$$

Here, the subscripts *sys*, *Au*, *rad*, *sat*, and *H* refer to the entire metal/SAM system, the pristine metal, the free-standing

molecular monolayer of radical and H-saturated species, and the layer of saturating H-atoms, respectively. Experimentally, ΔE_{BD} can be extracted from $\Delta\Phi$ measurements on a series of molecules with the aid of their calculated dipole moments and reasonable estimates for all other quantities in Eq. 2.[4-7]

Notably, DFT calculations pursuing the *saturated* approach have found values of $\Delta E_{BD} \approx$ -1.2 eV for SAMs of biphenylthiols on Au(111),[1-3] while negligible values (-0.01 – 0.08 eV) have been reported for SAMs of alkylthiols following the *radical* scheme.[9] Even more strikingly, experimental studies on thiols with an aromatic ring adjacent to the –SH group have reported a ΔE_{BD} of -0.85 eV when relying on μ values calculated for *saturated* molecules,[5] while a ΔE_{BD} between +0.6 and +1.0 eV has been found using μ values calculated for *radicals*.[6] Thus, the bond dipole of thiols on gold appears to depend not only on the chemical structure of the molecular backbone but, rather unsatisfactorily, also on

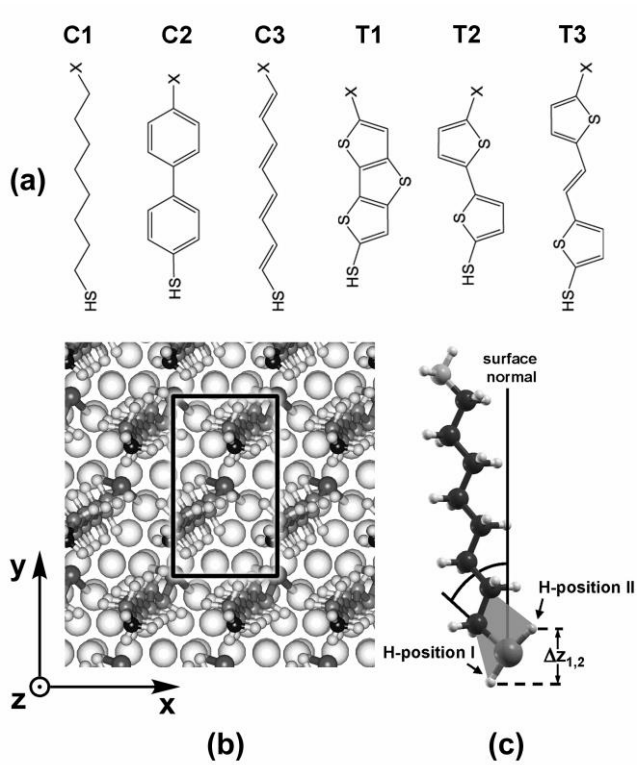

Fig. 1 (a) Chemical structures and labels of the investigated thiols; X stands for amino (–NH_2) and cyano (–CN) head-group substitutions. (b) Top view of the p(√3×3) surface unit cell containing two molecules (shown for C1), which is assumed for all SAMs. (c) Side view of one NH_2-substituted C1 molecule in the free-standing H-saturated monolayer indicating the two possible hydrogen positions, the inclination of the S–C bond to the surface normal, and the height difference, $\Delta z_{1,2}$, between the two saturating hydrogen atoms in position I and II.

the chosen partitioning scheme. It is the purpose of the latter, however, to permit correlating the chemical structure of the SAM-forming molecules with the achievable $\Delta\Phi$, thus allowing for the rational design of suitable molecules. Therefore, the question arises which of the two possibilities is better suited to provide a chemically and physically insightful picture of the relevant interfacial processes.

To elucidate this question, we performed slab-type DFT band-structure calculations for a series of functionalized thiols on Au(111) using VASP,[11] the internal-coordinate geometry optimizer GADGET,[12] and XCRYSDEN[13] (for details see ESI†). As shown in Fig. 1a, each molecule is endowed with a strongly polar head-group substitution that either lowers Φ in the case of the electron-donating amino group (–NH_2) or increases Φ in the case of the electron-accepting cyano group (–CN);[14] note that the total dipole moments of these molecules are composed of the contributions from the head groups on one side and from the thiol groups on the other side, the latter pointing roughly in the direction of the S–H bonds (*vide infra*). An in-depth analysis of the electronic properties of the molecules shown in Fig. 1a as well as the corresponding SAMs is provided in Ref. [14]. For the sake of comparability, the same rectangular p(√3×3) unit cell containing two molecules is assumed for all monolayers (Fig. 1b). To individually access all components in Eqs. 4, separate calculations were performed on the corresponding sub-systems listed there.

Table 1 DFT-calculated vertical distance, $\Delta z_{1,2}$, between the saturating hydrogen atoms in positions I and II,‡ left-sided ionisation potential, IP_{left}, energy perturbation of the highest occupied delocalized orbitals upon metal-molecule bonding, E_{corr}, and potential energy step due to the bond dipole, ΔE_{BD}, for hydrogen position I as well as ΔE_{BD} for hydrogen position II obtained for the saturated partitioning scheme.

		H-position			
		I			II
system	$\Delta z_{1,2}$ [Å]	IP_{left} [eV]	E_{corr} [eV]	**ΔE_{BD} [eV]**	ΔE_{BD} [eV]
C1-NH_2	1.919	7.74	0.03	**-1.27**	*0.16*
C1-CN	1.880	8.17	-0.01	**-1.00**	*0.13*
C2-NH_2	0.675	5.03	0.14	**-1.14**	*-0.69*
C2-CN	0.515	5.13	0.17	**-1.20**	*-0.85*
C3-NH_2	1.894	3.89	0.16	**-1.87**	*-0.78*
C3-CN	2.067	3.74	0.16	**-2.06**	*-0.88*
T1-NH_2	0.821	4.26	0.14	**-1.54**	*-1.01*
T1-CN	0.788	4.30	0.14	**-1.57**	*-1.07*
T2-NH_2	1.269	4.04	0.12	**-1.70**	*-0.94*
T2-CN	1.266	4.10	0.13	**-1.71**	*-0.95*
T3-NH_2	1.173	3.99	0.13	**-1.70**	*-0.98*
T3-CN	1.160	4.01	0.13	**-1.72**	*-1.02*

As it appears more natural and chemically intuitive (in contrast to R–S• radicals, the –SH terminated molecules are readily accessible to experiment), the *saturated* scenario is discussed first. There, when setting up the system for the free-standing molecular monolayer in order to determine ΔE_{vac} in Eq. 2 and ρ_{sat} in Eq. 4a, one is faced with the choice of where to place the hydrogen atom relative to the sulphur (Fig. 1c): Two positions can be identified, where the hydrogen lies in the plane defined by the sulphur and the two nearest carbon atoms. As the S–C bond is inclined to the surface normal by > 17° for all investigated molecules and the C–S–H bond angle is only ~97°, this results in the hydrogens to lie above the plane of the sulphur atoms in position II (*i.e.*, farther away from where the metal surface will be located once bonding is established), and below the sulphur plane in position I. As

ΔE_{BD} clearly should reflect the bonding of sulphur to gold, the latter position is obviously a better choice; one is primarily interested in the interfacial charge rearrangements *between* sulphur and gold and not in some spatial region within the molecular ad-layer, *i.e.*, where the saturating hydrogen atoms are located in position II (Fig. 1c). The ΔE_{BD} values obtained with the hydrogen at position I in the free-standing thiol layer are listed in Table 1. They are all negative and they reflect the local polarisability[14] of the molecular backbone adjacent to the sulphur to some extent, *i.e.*, larger values are observed for more polarisable backbones.[14] Notably, the value for the alkyl backbone C1 is non-zero. Also listed are the ΔE_{BD} values for hydrogen position II. Not only are they markedly different, but closer inspection of Table 1 reveals that the difference to the H-position I values increases essentially linearly with the height difference, $\Delta z_{1,2}$, between the hydrogens in the two positions (Fig. 1c), *i.e.*, with the projection of the local dipole moment around the –SH group onto the surface normal (*vide supra*);

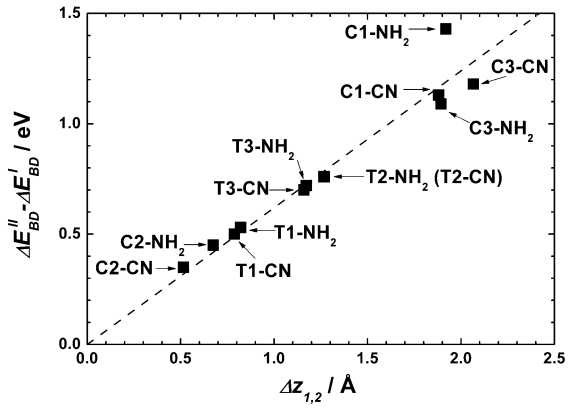

Fig. 2 Difference between the ΔE_{BD} values obtained with the saturated partitioning scheme for hydrogen positions I and II as a function of $\Delta z_{1,2}$, the height difference between the saturating hydrogen atoms in position I and II;‡ the dashed line is a linear fit through the origin.

the corresponding plot is shown in Fig. 2.‡ This indicates that, using the saturated partitioning scheme, ΔE_{BD} also reflects the position of the saturating H-atoms and, thus, the orientation of the S–C bond and the molecular plane with respect to the surface normal (Fig. 1c).

To test the ability of the saturated approach to provide chemically and physically insightful information, we also examined a different quantity, namely the "left-sided" ionisation potentials (*IP*s) of the free-standing saturated monolayers, which are defined as the energy difference between its highest occupied π-states (the highest fully delocalized σ-states in the case of C1)[14] and E_{vac} on the thiol side;[1-3] as the latter obviously differs from E_{vac} above the head-group substituents by ΔE_{vac}, also the "right-sided" *IP*s must differ from their left-sided counterparts by ΔE_{vac}.[1-3] Again, the IP_{left} values in Table 1 reflect the chemical nature of the molecular backbones, *i.e.*, lower values are found for structures with a more extended conjugation.[14] Similarly to ΔE_{BD}, IP_{left} also reflects the orientation of the S–C bond or, more precisely, the projection of the local dipole moment of the –SH group onto the layer normal (see ESI†).

Finally, it has been observed that the right-sided *IP*s in the free-standing monolayers differ from the *IP* of the SAM bonded to the metal (reported in Ref. [14]) by a small amount, E_{corr}, which reflects the perturbation of the molecular electronic structure through metal-molecule bonding.[1-3] As shown in Table 1, these E_{corr} values are below 0.2 eV for all investigated systems. This underlines that replacing the S–H bonds with S–Au bonds has little effect on the energy levels in the SAM and, again, the saturated partitioning scheme is seen to conserve the chemical information on the nature of the molecular backbone.

We now turn to the radical scenario where, instead of *replacing* S–H bonds with S–Au bonds, a new bond is *formed* between the R–S• species and the gold surface. While the radical is unlikely to actually participate in the process of SAM formation, one obviously needs not be concerned with the position of a saturating hydrogen atom on the sulphur. The

Table 2 DFT-calculated potential energy step due to the bond dipole, ΔE_{BD}, left-sided ionisation potential, IP_{left}, and energy perturbation of the highest occupied delocalized orbitals upon metal-molecule bonding, E_{corr}, obtained for the radical partitioning scheme.

system	ΔE_{BD} [eV]	IP_{left} [eV]	E_{corr} [eV]
C1-NH_2	-0.04	8.95	-0.02
C1-CN	-0.04	9.07	-0.09
C2-NH_2	1.11	6.07	-1.11
C2-CN	0.96	6.08	-1.08
C3-NH_2	1.33	6.11	-0.86
C3-CN	1.28	6.14	-0.83
T1-NH_2	1.28	5.89	-1.11
T1-CN	1.19	5.88	-1.07
T2-NH_2	1.22	5.81	-1.07
T2-CN	1.17	5.81	-1.08
T3-NH_2	1.27	5.89	-0.99
T3-CN	1.23	5.89	-0.99

results obtained with the radical partitioning scheme are listed in Table 2. In agreement with previous studies following this approach,[9] a vanishing ΔE_{BD} is found for the alkyl backbone C1 and, for all other molecular structures, ΔE_{BD} changes sign compared to the saturated scheme (Table 1); a potential dependence on the orientation of the S–C bond is hard to assess. Notably, the IP_{left} values in the radical case (Table 2) all lie within the narrow range of 5.8 – 6.1 eV (cf. Ref. [8]); the exception is again C1 due to the different nature (σ-orbital *vs.* π-orbital) of the highest occupied delocalized states.[14] Additionally, the E_{corr} values are on the order of 1 eV, yet again with the exception of C1 (*vide infra*). This leads to the conclusions that, in the radical partitioning scheme, chemical information on the nature of the backbone is largely lost and the electronic structure of the free-standing radical layer is significantly perturbed upon bonding to the metal.

The reason for these observations is that the radical character of the –S• termination dominates the electronic structure of the free-standing monolayer on the docking-group

side and, consequently, also the interfacial charge redistributions upon metal-molecule bond formation. Removing the hydrogen from the sulphur in the thiol and, thus, converting the closed-shell molecule into a radical, induces major charge rearrangements on that side of the molecule. The latter can be expressed as (ρ_{rad} + ρ_H) - ρ_{sat} and are shown in the left panels of Fig. 3 (grey). For all conjugated systems (C2 – T3), the charge redistributions resulting from hydrogen removal reach far onto the molecular backbones, as the sulphur is strongly coupled to their π-electron system. A qualitatively different behaviour is observed in the case of the alkylthiol (C1), where both the π-system and the radical character are strongly localized on the sulphur alone and, therefore, the delocalized σ-states are hardly affected by radical formation. When the bonds between radicals and gold are formed, *i.e.*, when charges are shifted according to Eq. 4b, the molecule is essentially converted back to a closed-shell species and the aforementioned charge redistributions are largely reversed in the spatial region of the SAM (left panels

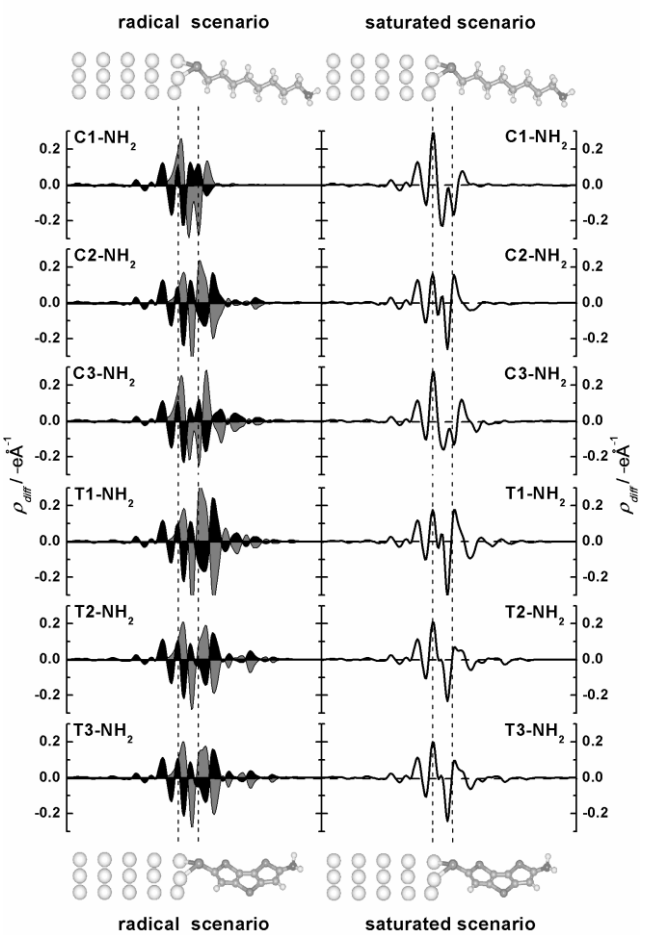

Fig. 3 (left panels) Plane-integrated charge-density difference per unit-cell area, (ρ_{rad} + ρ_H) - ρ_{sat}, describing the removal of the hydrogen from the thiol (grey) and plane-integrated charge-density difference per unit-cell area, ρ_{diff} after Eq. 4b, describing the bond formation between radical and metal (black). (right panels) Plane-integrated charge-density difference per unit-cell area, ρ_{diff} after Eq. 4a, describing the bonding of the hydrogen-saturated molecular monolayer to the metal. The curves in the right panels, which describe the actual bonding-induced interfacial charge rearrangements, are also the sum of the two curves in the left panel. The vertical lines indicate the (average) positions of the top-most gold layer and the sulphur atoms.

in Fig. 3, black), but not quite. The actual chemical and physical information regarding the bonding lies hidden in the *difference* between the processes of removing the hydrogen atoms from the sulphur and "adding" the gold surface instead. Exactly this difference (right panels in Fig. 3), which actually corresponds to ρ_{diff} in the *saturated* partitioning scheme (Eq. 4a), is obscured in the radical approach.

To summarize, we have identified and discussed two distinctly different ways of defining the Au–S bond dipole in thiol SAMs on Au(111), the saturated and the radical scheme. With a well-defined choice for the positions of the saturating hydrogen atoms on the sulphur, the former conserves information on the chemical structure of the thiols, reflects the orientation of the S–C bond, and provides revealing insights into the interfacial charge rearrangements that occur upon metal-molecule bonding. In particular, a considerable negative ΔE_{BD} is found for a wide range of molecules, including alkylthiols. On the other hand, when considering unsaturated R–S• species as the origin of the molecular contribution to the work-function modification, chemical information on the SAM electronic structure is largely lost and the relevant bonding-related charge redistributions at the metal/molecule interface are not accessible, which clearly renders this second approach less appealing.

This work was supported by the National Natural Science Foundation of China, the Ministry of Science and Technology of China through the 973 program (Grants 2006CB806200, 2006CB932100), by the FWF through project P20972-N20, and by the DFG through the Sfb448 "Mesoscopically Organized Composites".

Notes and references

[a] *Department of Chemistry, Tsinghua University, 100084 Beijing, PR China. Fax: +86/10/6279-7689; Tel: +86/10/6279-7689; E-mail: zgshuai@tsinghua.edu.cn*
[b] *Institute of Solid State Physics, Graz University of Technology, Petersgasse 16, A-8010 Graz, Austria. Fax: +43/(0)316/873-8466; Tel: +43/(0)316/873-8475; E-mail: egbert.zojer@tugraz.at*
[c] *Key Laboratory of Organic Solids, Beijing National Laboratory for Molecular Sciences (BNLMS), Institute of Chemistry, Chinese Academy of Sciences, 100190 Beijing, PR China*
[d] *Institut für Physik, Humboldt-Universität zu Berlin, Newtonstr. 15, D-12489 Berlin, Germany*

† Electronic Supplementary Information (ESI) available: Additional computational results on the properties of the free-standing molecular monolayers. See DOI: 10.1039/b000000x/

‡ As there are two inequivalent molecules per unit cell (Fig. 1b), the average $\Delta z_{1,2}$ values are reported.

1 G. Heimel, L. Romaner, E. Zojer and J. L. Bredas, *Acc. Chem. Res.*, 2008, **41**, 721.
2 G. Heimel, L. Romaner, E. Zojer and J. L. Bredas, *Nano Lett.*, 2007, **7**, 932.
3 G. Heimel, L. Romaner, J. L. Bredas and E. Zojer, *Surf. Sci.*, 2006, **600**, 4548.
4 B. de Boer, A. Hadipour, M. M. Mandoc, T. van Woudenbergh and P. W. M. Blom, *Adv. Mater.*, 2005, **17**, 621.
5 M. Malicki, Z. Guan, S. D. Ha, G. Heimel, S. Barlow, M. Rumi, A. Kahn and S. R. Marder, *Langmuir*, 2009, **25**, 7967.

6 R. W. Zehner, B. F. Parsons, R. P. Hsung and L. R. Sita, *Langmuir*, 1999, **15**, 1121.
7 I. H. Campbell, S. Rubin, T. A. Zawodzinski, J. D. Kress, R. L. Martin, D. L. Smith, N. N. Barashkov and J. P. Ferraris, *Phys. Rev. B*, 1996, **54**, 14321; I. H. Campbell, J. D. Kress, R. L. Martin, D. L. Smith, N. N. Barashkov and J. P. Ferraris, *Appl. Phys. Lett.*, 1997, **71**, 3528; D. M. Alloway, M. Hofmann, D. L. Smith, N. E. Gruhn, A. L. Graham, R. Colorado, V. H. Wysocki, T. R. Lee, P. A. Lee and N. R. Armstrong, *J. Phys. Chem. B*, 2003, **107**, 11690.
8 Q. Sun and A. Selloni, *J. Phys. Chem. A*, 2006, **110**, 11396.
9 P. C. Rusu and G. Brocks, *Phys. Rev. B*, 2006, **74**, 073414; P. C. Rusu and G. Brocks, *J. Phys. Chem. B*, 2006, **110**, 22628; V. De Renzi, R. Rousseau, D. Marchetto, R. Biagi, S. Scandolo and U. del Pennino, *Phys. Rev. Lett.*, 2005, **95**, 046804.
10 L. Romaner, G. Heimel and E. Zojer, *Phys. Rev. B*, 2008, **77**, 045113; L. Romaner, G. Heimel, C. Ambrosch-Draxl and E. Zojer, *Adv. Funct. Mater.*, 2008, **18**, 3999.
11 G. Kresse and J. Furthmüller, *Phys. Rev. B*, 1996, **54**, 11169; G. Kresse and J. Furthmüller, *Comp. Mater. Sci.*, 1996, **6**, 15; G. Kresse and D. Joubert, *Phys. Rev. B*, 1999, **59**, 1758.
12 T. Bučko, J. Hafner and J. G. Angyan, *J. Chem. Phys.*, 2005, **122**, 124508.
13 A. Kokalj, *Comp. Mater. Sci.*, 2003, **28**, 155. Code available from http://www.xcrysden.org/.
14 L. J. Wang, G. M. Rangger, L. Romaner, G. Heimel, T. Bucko, Z. Y. Ma, Q. K. Li, Z. Shuai and E. Zojer, *Adv. Funct. Mater.*, 2009, **19**, 3766..